Indoor Positioning with Ultra-Wideband: Enhancing Accuracy through Data Filtering

Laura Vaccari*, Antonio Maria Coruzzolo*, Francesco Lolli*,,***, Bianca Rimini***

** Department of Sciences and Methods for Engineering, University of Modena and Reggio Emilia, Via Amendola 2, 42122, Reggio Emilia, Italy (laura.vaccari@unimore.it, antoniomaria.coruzzolo@unimore.it, bianca.rimini@unimore.it)*

*** Interdepartmental Centre En&Tech, Piazzale Europa, 1, 42124, Reggio Emilia, Italy(francesco.lolli@unimore.it,)*

**** Interdepartmental Centre InterMech MO.RE, University of Modena and Reggio Emilia, Piazzale Europa, 1, 42124, Reggio Emilia, Italy*

Abstract: Indoor positioning technology plays a vital role in tracking movements within spaces where traditional outdoor GPS systems fail to operate effectively. This research employed Ultra-Wideband (UWB) technology to monitor the live trajectory of operators within an actual production facility. The system's effectiveness was assessed in two key zones: the goods receiving and shipping area, and the space amidst warehouse shelves. Enhanced results were achieved through the implementation of various filtering techniques. Nonetheless, the study also uncovered practical limitations, revealing a level of accuracy lower than expected.

Keywords: Indoor Positioning, Warehouse, UWB, Tracking, Real-time

1. Introduction

There are many people tracking systems to be exploited in different environments, such as warehouses, hospitals, schools, farms, and supermarkets. These systems localize movements within structures, where GPS technologies applied to outdoor environments cannot function. Indoor positioning technology is used to track the movements of goods, operators, or vehicles (Barral et al. 2019b), to detect incidents and ensure worker safety (Singh, Kalaichelvi & Karthikeyan 2023a), to manage warehouse activities and logistical operations, including order-picking activities (Zadgaonkar & Chandak 2021), defining routes (Okumuş, Dönmez & Kocamaz 2020), bottleneck identification or rylayout. Other fields of application are the geolocation of people (Liao et al. 2016), items (Sun & Ma 2017), robots (Murdan & Emambocus 2018), AGVs (Zhang Xinand Wang, 2013), or UAVs (Jin et al. 2023). The tracking methods can be light-based (Jung & Song 2017), sound-based (Gabbrielli et al. 2023), or radio frequency-based (Khan, Kai & Gul 2017). From the literature, there has been a significant contribution of radio frequency-based technologies, particularly RFID technology, which is the most widely used. The tag's position calculation approaches are diverse: computer-based (Ooi, Lee & Chea 2018), constraint-based (Khalaf-Allah 2020), fingerprinting (Torteeka, Chundi & Dongkai 2014), geometric methods (Gnaś & Adamkiewicz 2022) or self-processing (Singh, Kalaichelvi & Karthikeyan 2023b). The data used by those different approaches are image-based (Jung & Song 2017), signal characteristic-based (Torteeka et al. 2014), time-based (Singh, Kalaichelvi & Karthikeyan 2023c), angle-based (Singh et al. 2023b) or motion-based (Silva, Pendao & Moreira 2022). Using any localization method, accuracy will never be one hundred per cent. For this reason, filters can be used to improve the results obtained from the sole use of indoor positioning devices. Filters can be machine learning-based (Xiang et al. 2019), particle filters (Khalaf-Allah 2020), clustering methods (Abed & Abdel-Qader 2019), or other mathematic approaches, among these the most used filter is the Kalman filter (Barral et al. 2019b). UWB is a radio frequency-based technology that enables continuous real-time indoor tracking with higher accuracy than other radio frequency-based technologies (Barral et al. 2019b; Sartayeva et al. 2023) In our study, we used UWB technology with geometric approaches, particularly trilateration, and chose Pozyx with time-based data such as TDoA (time difference of arrival) and Twr (Two Way ranging) to track the real-time movement of operators in the warehouse. As filters, we used median smoothing, exponential smoothing and mixed filters. Few studies have tested UWB in real-world scenarios, as in (Barral et al. 2019a; Gnaś & Adamkiewicz 2022; Singh et al. 2023a), in contrast to the extensive research available on RFID. We aim to bridge this gap through our study that aims to assess the accuracy of UWB technology in a warehouse by tracking the movements of warehouse operators within a company. The study will highlight the strengths and weaknesses of this technology in a real word environment.

2. Methodology

The chosen tool to track the operator's real-time movement within the company warehouse is the Pozyx creator kit, a UWB system. The kit consists of five anchors and four tags, as shown in Figure 1 and Figure 2 respectively. Each tag moves along with the operator, a worker or a forklift, to detect its position relative to the anchors. The chosen method for position calculation is trilateration, which uses basic geometry and determines the tag's position by

measuring the distance from the tag to three anchors. The tag's position is uniquely identified by the intersection of the three circles formed around the anchors. The data obtained from the tags and anchors include TWR and TDoA. The test was conducted on two distinct areas: the Modula's area,the area in front of a two-unit vertical warehouse (Figure 3), and the shelving area (Figure 4). The computer with a tag was positioned in the centre of the area, and manual calibration was carried out by entering the coordinates of the anchors relative to the selected origin. The coordinates for the first setup are shown in Table 1, and those for the second setup are shown in Table 2. The Modula's area covers $25.8 \times 18.5 = 487\ m^2$. In this area five anchors were positioned within a maximum distance of 20 meters from each other (Figure 3). The shelving area is the area between two shelves, this area is five times smaller than the Modula's area and covers $15.41 \times 3.4 = 52\ m^2$ (Figure 4). Here the distance between each anchor is at most four meters. However, the narrow and elongated geometry does not allow all the anchors to always have a line of sight (LOS), making localization challenging. It was necessary to reposition the anchors between two shelves because the signal would not have been accurate if a shelf had been placed in between. Modula's and Shelving areas typically contain an average of five people walking inside, two forklifts, and pallets loaded with materials positioned on the floor, all of these elements cause interference and non-line of sight (NLOS) between the anchors. In Figure 3 and Figure 4 red lines represent NLOS between anchors, while green lines represent LOS. The greater the number of anchors, the higher the accuracy of the system, but also the cost. For this reason, a compromise had to be reached. Afterwards, by changing the host, topic, username, and password, it was possible to connect to the Pozyx cloud via the MQTT protocol and collect position data for the different two setups. Numerous tests were conducted in the two previously mentioned areas on different sampling days. After collecting the positioning data, it was necessary to improve them using filters. Filters were applied through the implementation of Python code written in Microsoft Visual Studio Code.

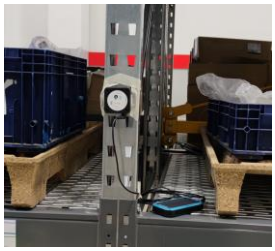

Figure 1: Anchor

Figure 2: Tag 7633

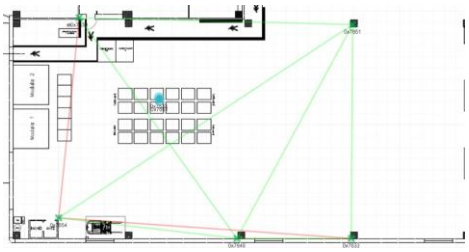

Figure 3: Modula's Map. *The two vertical warehouses are represented by the two rectangles on the left. Anchors are represented by green crosses and tags by blue circles.*

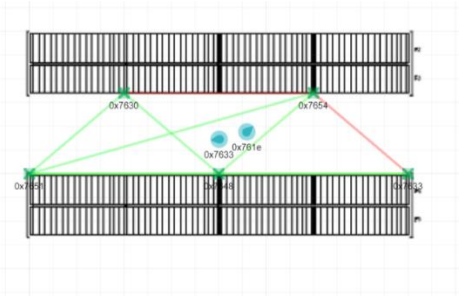

Figure 4: Shelving Map. *Anchors are represented by green crosses and tags by blue circles.*

Table 1: Modula Setup (mm)

Tag ID	X	Y
7630	1800	19400
7633	25770	0
7648	15700	0
7651	25900	18800
7654	0	1800

Table 2: Shelver Setup (mm)

ID	X	Y
7630	4200	3400
7633	15413	0
7648	8147	0
7651	740	0
7654	12462	3400

3. Filters

The displayed paths were obtained from processing the data collected by using filters. Filters are needed to have better accuracy, (Barral et al. 2019b). The applied filters included threshold, median smoothing, exponential smoothing and a mixed one.

3.1 Threshold filter

The raw data was modified by initially applying a "threshold" filter. It aims to eliminate duplicate points, as a matter of fact in our study, the tag was detected many times

in the same location on the warehouse map, distorting the actual path. For instance, when taking one of the paths, the percentage of duplicates was 64%, so removing them was crucial for cleaning the data. It also deletes points that are disproportionately distant from their preceding and succeeding points, compared to the time elapsed between their detections. In our study, if the distance measured between a point and its preceding and succeeding points was greater than one meter, then it was considered excessive, and the central point was eliminated. After all, the operator cannot have travelled 1 meter in $\frac{1}{20}$ of a second, as data were collected at 20 Hz frequency.

3.2 **Median smoothing filter**

The "median smoothing" filter computes an average for each point using the four preceding and succeeding points for both x and y coordinates, as shown in Equation 1 for coordinate x.

$$x[k] = \frac{cx[k]+(\sum_{i=1}^{i=4} cx[k+i]+cx[k-i])}{9} \quad (1$$

where $x[k]$ is the filtered value for period $[k]$, $cx[k]$ is the value detected by Pozyx for period k$(t = k)$. In this case, every detected value has the same weight as the others.

3.3 **Exponential smoothing filter**

The "exponential smoothing" filter returns a data point that is a combination of the detected data and the forecast made in the previous points, as shown in Equation 2 for coordinate x. The same has to be calculated for coordinate y. This filter utilizes the previous forecast for the present and actual data to predict the next point with a weighted average. The weights exponentially decrease for past values.

$$x[k+1] = 0.7 \times cx[k] + (1-0.7) \times x[k] \quad (2$$

where x is the forecast, $cx[k]$ is the present value for period k $(t = k)$, and 0.7 is the parameter alfa α determining how much the future forecast is based on present data or past forecasts. In this case, the forecast $x[k+1]$ relies more on data based on the detected value $cx[k]$ rather than the forecast $x[k]$. The Equation 1 can be written also as the Equation 3, where the future prediction is a weighted average of all past values, with weights decreasing exponentially.

$$x[k+1] = \sum_{i=0}^{i=k} 0.7 \times (1-0.7)^i \times cx[k-i] \quad (3$$

3.4 Mixed filter

Another type of filter, known as Mixed, employs the equation of exponential smoothing (Equation 2) with α value set to 0.3. As input data, it uses the output coordinates from the median smoothing equation.

4. **Results**

The results obtained from applying the code to the data collected by Pozyx are measured in terms of accuracy. The traced path is compared to the ground truth path, the latter was defined by applying a mark on the ground to be carefully followed. Filters were applied to modify the traced path of each tag and make it closer to the ground route path. To measure accuracy, several tests were conducted to assess how precise the system is in defining the position of the tag in the two areas of the warehouse.

4.1 **Accuracy calculation**

Accuracy is measured as Mean Absolute Error (MAE), which is the average of the distances between all points and their real counterparts, as calculated in Equation 4.

$$MAE = \frac{1}{n}\sum_{i=1}^{n}|\hat{y}_i - y_i| \quad (4$$

where $\hat{y}_i$ are the predicted values, y_i are the observed values, and n is the number of observations. The first step is to calculate the distance from the detected point to the real point where the operator passed. The actual path taken was marked on the ground with adhesive tape, and through Python code, the distance was calculated using the projection of the point onto the line. To calculate the distance from the actual line, it is necessary to define its angular coefficient m and its parameter q, using two points on the line $P_2(x_2, y_2)$ and $P_1(x_1, y_1)$, through Equation 5 and 6.

$$m = \frac{(y_2-y_1)}{(x_2-x_1)} \quad (5$$

$$q = y_1 - m \times x_1 \quad (6$$

The second step is to calculate the point on the actual line $A(x, y)$ where the detected point $A_2(A_x, A_y)$ should be, using the fEquation 7 and Equation 8. Finally, the Pythagorean theorem is applied to calculate the distance between the actual point and the point detected by Pozyx, using Equation 9.

$$x = \frac{(A_x+A_y\times m-q\times m)}{(m^2+1)} \quad (7$$

$$y = \frac{(A_x\times m+A_y\times m^2-q\times m^2)}{(m^2+1)} + q \quad (8$$

$$distance = \sqrt[2]{(A_x - x)^2 + (A_y - y)^2} \quad (9$$

4.2 **Test settings**

Many filtered data are shown in Figure 5, Figure 6, Figure 7: the yellow line is the raw data, the green line is the threshold filtered data, the blue line is the exponential smoothing filtered data, the red line is the median smoothing filtered data and finally the black line is the mixed filtered data. The first setup was designed by applying five points on the ground and traversing a rectangle, Figure 5, and a triangle, Figure 6. On the upper side of the rectangle, the data were not correctly detected due to metallic interferences placed in the middle of the area. As seen in Figure 5, the unfiltered data deviate from reality, and even the paths in green and blue show a deviation from reality for a few points. Mixed and median smoothing filters were influenced by this wrong data and they did not eliminate the wrong deviation but rather rounded it off causing the creation of further erroneous points. Indeed, the negative aspect of averaging, which results in a rounding of the curve, is that it would be accurate to have sharp edges to reflect the actual path. In the shelving area, the second setup, several tests were conducted. The first test involved assessing the quality of

the Pozyx system by traversing a triangle in the corridor between two shelves, as shown in Figure 7.

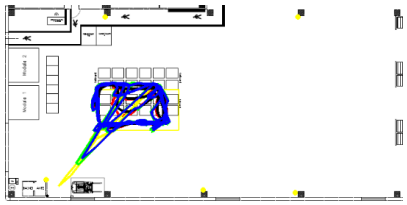

Figure 5: Rectangular path

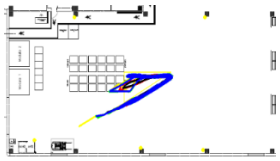

Figure 6: Triangular path

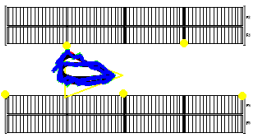

Figure 7: Shelving path

4.3 Accuracy results

Table 3 presents the accuracy results of the tests conducted in the warehouse, calculated using the MAE. Each row corresponds to a different path, and the accuracy varies based on the filter used, indicated in the respective column. P is a path, so it can be in the Modula zone (M), the central part of the Modula zone (C), or the shelving zone (S). The filters applied to the raw data R are: MI for mixed, M for median smoothing, E for exponential smoothing, and T for threshold. In addition, AM, AC and AS are the average accuracy values among all paths for each filter in the Modula zone, central Modula zone and shelving zone, respectively. Lastly, A is an average of the line. Tot A is the average for all the tests of each filter. For example, the accuracy results of the example in Figure 5 are in Table 3 in line M2, where the exponential smoothing has the best result. The accuracy results of the example in Figure 6 are in Table 3 in the line C2 where all the filters have roughly the same accuracy. The accuracy measured in the shelving area of the path shown in Figure 7 is in line S4 in Table 3.

Table 3: MAE-filters-accuracy(cm)-paths

P	MI	M	E	T	R	A
M1	42.2	45.1	37.3	37.7	42.5	40.96
M2	57.4	56.9	55.2	56.1	60.9	57.3
M3	109.2	105.6	98.7	95.7	100.7	101.98
M4	63.5	61.7	60.29	60.2	60.29	61.19
M5	82	78	75.2	75.7	75.9	77.36
AM	70.86	69.46	65.33	65.08	68.05	67.75
C1	59.5	60.1	61.8	62.4	61.7	61.1
C2	62.8	62.43	62.5	62.45	63.9	62.81
C3	48.8	46.7	46.62	46.61	55.4	48.82
C4	57.3	57.5	57.4	57.2	57.6	57.4
AC	57.1	56.68	57.08	57.16	59.65	57.53
S1	18.66	18.9	18.4	18.81	18.81	18.71
S2	18	18.9	19.83	19.87	19.87	19.29
S3	16.14	17.12	17.8	18.13	18.13	17.46
S4	22.2	22.5	23	23.25	23.25	22.84
S5	18.87	18.74	19.42	19.67	19.67	19.27
AS	18.77	19.23	19.69	19.94	19.94	19.51
Tot A	48.32	47.87	46.67	46.69	48.47	

From the results in Table 3, it can be observed that the average accuracy greatly depends on the area in which the path is conducted: Modula, Central Modula, or shelving area. The average accuracy of these areas is 67.75, 57.53, and 19.51, respectively, highlighting that the accuracy range is almost tripled in the Modula area compared to the shelving area, which have an area nine times smaller. Furthermore, in the first area, the filters with the best average results are Exponential Smoothing (65.33) and Threshold (65.08) filters, in the second area, they are Median Smoothing (56.68) and Exponential Smoothing (57.08), and finally, in the shelving area, they are Mixed (18.77) and Median Smoothing (19.23) filters. Overall, the filters that performed best are Exponential Smoothing (46.67) and Threshold (46.69). Table 4 shows the percentage differences in accuracy achieved with a filter compared to the best (lowest) accuracy in that particular path. These values are calculated using the accuracies from Table 3. This calculation is performed for each row, meaning for each path. The average has been calculated for the module zone (AM), for the central area of the warehouse (AC), and for the shelving area (AS), obtaining respective average relative performance differences of the filters of 5%, 2%, and 5%. Indeed, in Table 4, it can be noted how, on average, the filters act uniformly. Furthermore, it can be observed that if the percentage in the raw data column (R) is high, then it means that the filters have correctly acted by modifying the collected raw data.

Table 4: Percentage relative differences - %

P	L	M	E	T	R	
M1	13	21	0	1	14	
M2	4	3	0	2	10	
M3	14	10	3	0	5	
M4	5	2	0.1	0	0.1	
M5	9	4	0	1	1	
AM						5%
C1	0	1	4	5	4	
C2	1	0	0.1	0.03	2	
C3	5	0.1	0.02	0	18	
C4	0.1	0.5	0.3	0	0.6	

AC						2%
S1	1	3	0	2	2	
S2	0	5	10	10	10	
S3	0	6	10	12	12	
S4	0	1	3	4	4	
S5	0.6	0	3	4	4	
AS						5%

5. **Management applications**

The management applications include data related to marked areas within the warehouse. It is desired to determine if the tag has passed through them and how many times, in order to construct a From-To chart matrix. The company's warehouse is divided into three marked areas: the unloading zone (black area in Figure 8) where materials are received from external suppliers, the storage area in the two Modula units (yellow area in Figure 8), and the input zone (blue area in Figure 8) where materials are prepared for storage upon receipt or before shipping. The From-To chart vector defines the zones where the operator has passed through; the time interval chosen to record the tag's location is every five seconds, implying that the operator is walking quickly from one zone to another. As shown in Figure 8 and Table 5, the operator started from the unloading zone(U), then passed to the Modula area(M), the input zone(I), the Modula area(M) again and finally the input zone(I).

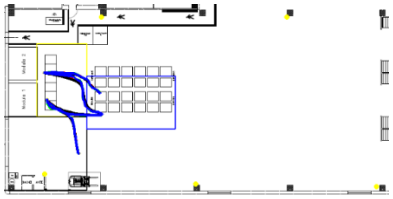

Figure 8: Markers' zones

Table 5: From-To matrix

From/to	U	M	I
U	X	1^	
M		X	2^,4^
I		3^	X

With the From-To matrix information, we can create a heatmap to highlight the most visited areas of the warehouse. The heatmap is a graphical representation where the colours indicate the areas most frequented by the warehouse operator, with the hottest and darkest colors representing the highest frequency. In this example (Figure 9), the coloured rectangle has been visited at least once, and the darker colour indicates the most visited areas, as explained in the "Wistia" colour legend in the upper-left part of the figure. The operator spent nearly 35 minutes consistently in front of the Modula's vertical warehouse, indicated by the orange colour, storing materials. By using this heatmap, it is possible to gather information about the possible presence of bottlenecks. All of this information can be used to enhance logistics and reconfigure the layout if necessary.

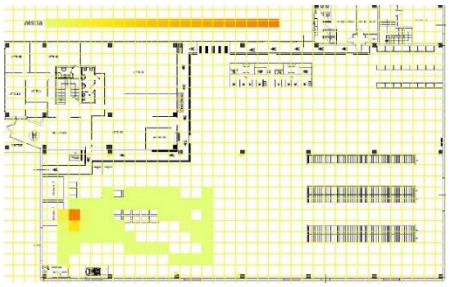

Figure 9: Heat-map

By monitoring the paths of operators inside the warehouse, excessive movements or time-consuming travel distances can be identified, which can then be optimized to improve the working environment. Two 30-minute experiments were conducted, in which the operator had to store the material from the unloading zone to the shelving area (Figure 10) or from the unloading zone to the Modula's area (Figure 11). The operator's path is represented by the red line, after applying the median smoothing filter. In Figure 11, it can be noticed how, after the modification of the layout, the operator has a shorter distance to travel to reach the warehouse area from the unloading zone during merchandise allocation. This streamlines the process, as the merchandise is directly stored in the Modula upon receipt from the truck. The use of the Pozyx device allows the calculation of distances travelled, improving the efficiency of the warehouse.

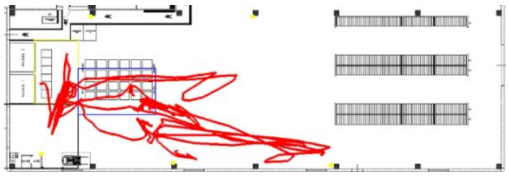

Figure 10: Shelving warehouse

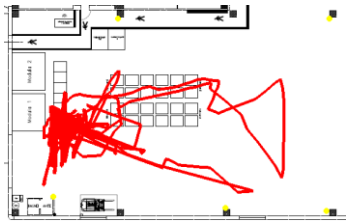

Figure 11: Modula warehouse

The second output obtained from using the Python code is the percentage of points not detected by Pozyx due to interference. The ideal condition is that the anchors and tags of the creator kit collect data at a frequency of 20 Hz, meaning 20 positions per second, but unfortunately, the percentage of detected data is never fully met. The third output is the percentage of points eliminated due to excessive distances, while the fourth output is the percentage of points eliminated because they are duplicates, as they were both explained before in the threshold filter part. The fifth output is the distance travelled by the

operator traced by the tag, using the x and y coordinates detected by Pozyx calculating the Pythagorean theorem. The sixth output is the elapsed time of the travel converted from a timestamp value to a value in seconds. The seventh output is the average speed, which is calculated using the space and time data. Lastly, the final output is the visualization of the path on the Pygame window projected onto the real map of the warehouse where the tests were conducted, as shown in Figure 8.

6. **Discussion**

The Ultra-Wideband (UWB) technology has been gaining attention in recent years due to its exceptional capabilities in indoor positioning systems. UWB technology offers several advantages over other technologies, such as Bluetooth, WiFi, and RFID which have lower accuracy.

Our study revealed that the placement of anchors and the movement of tags significantly affect path accuracy. The environment can have different physical, (Vui & Nordin 2014), and electromagnetic interferences, (Silva et al. 2022): physical obstacles, electromagnetic sources, objects in movement, changes in the radio frequency environment, and absorbing materials, all of these can affect the accuracy of measurements.

In our study, we identified several obstacles that can affect the functioning of the geolocation system. These include interferences and signal loss caused by excessive distances between the anchors or physical obstacles. The accuracy of our results, remained at approximately 60 cm in the Modula area and 20 cm in the shelving area, this difference in accuracy was probably due to physical obstructions, especially metallic ones, as in (Bartoletti et al. 2018). The difference in accuracy could also be attributed to the larger distance between anchors in the Modula area, which covers a greater space. Indeed, we noticed a significant improvement in accuracy when the anchors were placed closely together, such as in the shelving area where the anchors were 4 meters apart. Deploying a large number of anchors to monitor the entire facility simultaneously would lead to better results to a significant increase in costs. In this paper, various filters were applied and the results were than compared to each other. There was not a significant improvement in using one filter over another; however, on average, all filters yielded better results compared to the raw data (Tot A in Table 3). This led us to the conclusion that the accuracy depends on the environmental features, as the filters consistently produced results very close to each other.

Several studies tested UWB technology in various environments, using different techniques. In (Barral et al. 2019b), Pozyx technology was utilized to track a forklift in 20x20 areas of a warehouse, achieving real-time positioning accuracy of up to 13 cm. These results were obtained by employing a neural network, as well as inertial and optical sensors in addition to Pozyx, and then applying an extended Kalman filter to the data. The Pozyx system used in another study (Singh et al. 2023a) was tested in a warehouse of 5.6 * 11.3 m, with minimal interference. The authors used machine learning filters for sensor fusion, not only time of flight data from Pozyx but also inertial data, achieving a mean absolute error of 8 cm. In addition, Gnaś & Adamkiewicz, (2022) tested UWB technology in a university room 5*5 using the trilateration system and achieved an accuracy between 10 and 40 cm.

We could improve accuracy by incorporating additional sensors, and applying different filters.

This study has some limitations. Firstly, the number of tested paths was limited, which might not adequately represent the variety of real-world scenarios. Additionally, only two specific setups were considered, reducing the generalizability of the results. To address these limitations, future research should test a wider range of areas with different characteristics and use a greater variety of setups to enhance the robustness of the conclusions.

7. **Conclusion**

The performance of UWB localization techniques heavily depends on the setup and specific interferences present in the testing environment. The analyzed filters have been shown to increase the overall accuracy of measurements, with performance remaining quite similar among them. However, the exponential smoothing filter appears to be the best in terms of performance. Our results are similar to those reported in the literature, (Barral et al. 2019b), (Singh et al. 2023a), Gnaś & Adamkiewicz, (2022), and we can improve accuracy by utilizing additional inertial and optical sensors. Further investigations on better filtering and methods or different anchor placing points are needed to achieve better accuracy. Future managerial applications could include the use of UWB technology to create digital twins of warehouses. This approach would allow for more precise and efficient management of resources and operations within warehouses, thus improving the optimization of logistics processes and the ability to respond to changes in supply and demand.

References

Abed, A. & Abdel-Qader, I., 2019, 'RSS-Fingerprint Dimensionality Reduction for Multiple Service Set Identifier-Based Indoor Positioning Systems', *Applied Sciences*, 9(15).

Barral, V., Suárez-Casal, P., Escudero, C.J. & García-Naya, J.A., 2019a, 'Multi-sensor accurate forklift location and tracking simulation in industrial indoor environments', *Electronics (Switzerland)*, 8(10).

Barral, V., Suárez-Casal, P., Escudero, C.J. & García-Naya, J.A., 2019b, 'Multi-sensor accurate forklift location and tracking simulation in industrial indoor environments', *Electronics (Switzerland)*, 8(10).

Bartoletti, S., Decarli, N., Dardari, D., Chiani, M. & Conti, A., 2018, 'Order-of-arrival of tagged objects', *IEEE Journal of Radio Frequency Identification*, 2(4), 185 – 196.

Gabbrielli, A., Bordoy, J., Xiong, W., Fischer, G.K.J., Schaechtle, T., Wendeberg, J., Höflinger, F., Schindelhauer, C. & Rupitsch,

S.J., 2023, 'RAILS: 3-D Real-Time Angle of Arrival Ultrasonic Indoor Localization System', *IEEE Transactions on Instrumentation and Measurement*, 72, 1–15.

Gnaś, D. & Adamkiewicz, P., 2022, 'INDOOR LOCALIZATION SYSTEM USING UWB', *Informatyka, Automatyka, Pomiary w Gospodarce i Ochronie Srodowiska*, 12(1), 15–19.

Jin, Z., Zeng, Q., Li, Y., Sun, Y., Wang, H. & Li, B., 2023, *A Pose Estimation Method for Indoor UAV Based on Binocular Vision*, *2023 6th International Symposium on Autonomous Systems (ISAS)*, 1–6.

Jung, M. & Song, J.-B., 2017, 'Robust mapping and localization in indoor environments', *Intelligent Service Robotics*, 10(1), 55–66.

Khalaf-Allah, M., 2020, 'Particle filtering for three-dimensional tdoa-based positioning using four anchor nodes', *Sensors (Switzerland)*, 20(16), 1 – 27.

Khan, M., Kai, Y.D. & Gul, H.U., 2017, *Indoor Wi-Fi positioning algorithm based on combination of Location Fingerprint and Unscented Kalman Filter*, *2017 14th International Bhurban Conference on Applied Sciences and Technology (IBCAST)*, 693–698.

Liao, Y.-T., Chen, T.-L., Chen, T.-S., Zhong, Z.-H. & Hwang, J.-H., 2016, 'The Application of RFID to Healthcare Management of Nursing House', *Wireless Personal Communications*, 91(3), 1237–1257.

Murdan, A.P. & Emambocus, M.Z.A., 2018, *Indoor positioning system simulation for a robot using radio frequency identification*, *2018 13th IEEE Conference on Industrial Electronics and Applications (ICIEA)*, 986–991.

Okumuş, F., Dönmez, E. & Kocamaz, A.F., 2020, 'A cloudware architecture for collaboration of multiple agvs in indoor logistics: Case study in fabric manufacturing enterprises', *Electronics (Switzerland)*, 9(12), 1–24.

Ooi, B.-Y., Lee, W.-K. & Chea, K.-C., 2018, *Localization of Mobile Sensor Nodes Using QR Codes and Dead Reckoning with Error Correction*, *2018 21st International Conference on Electrical Machines and Systems (ICEMS)*, 841–845.

Sartayeva, Y., Chan, H.C.B., Ho, Y.H. & Chong, P.H.J., 2023, 'A survey of indoor positioning systems based on a six-layer model', *Computer Networks*, 237, 110042.

Silva, I., Pendao, C. & Moreira, A., 2022, 'Real-World Deployment of Low-Cost Indoor Positioning Systems for Industrial Applications', *IEEE Sensors Journal*, 22(6), 5386 – 5397.

Singh, A., Kalaichelvi, V. & Karthikeyan, R., 2023a, 'Machine learning-based multi-sensor fusion for warehouse robot in GPS-denied environment', *Multimedia Tools and Applications*.

Singh, A., Kalaichelvi, V. & Karthikeyan, R., 2023b, 'Machine learning-based multi-sensor fusion for warehouse robot in GPS-denied environment', *Multimedia Tools and Applications*.

Singh, A., Kalaichelvi, V. & Karthikeyan, R., 2023c, 'Machine learning-based multi-sensor fusion for warehouse robot in GPS-denied environment', *Multimedia Tools and Applications*.

Sun, E. & Ma, R., 2017, *The UWB based forklift trucks indoor positioning and safety management system*, *2017 IEEE 2nd Advanced Information Technology, Electronic and Automation Control Conference (IAEAC)*, 86–90.

Torteeka, P., Chundi, X. & Dongkai, Y., 2014, *Hybrid technique for indoor positioning system based on Wi-Fi received signal strength indication*, *2014 International Conference on Indoor Positioning and Indoor Navigation (IPIN)*, 48–57.

Vui, L.C. & Nordin, R., 2014, 'Lateration technique for wireless indoor positioning in single-storey and multi-storey scenarios', *Journal of Theoretical and Applied Information Technology*, 68(3), 670 – 675.

Xiang, C., Zhang, Z., Zhang, S., Xu, S., Cao, S. & Lau, V., 2019, *Robust Sub-Meter Level Indoor Localization - A Logistic Regression Approach*, *ICC 2019 - 2019 IEEE International Conference on Communications (ICC)*, 1–6.

Zadgaonkar, H. & Chandak, M., 2021, 'Locating Objects in Warehouses Using BLE Beacons Machine Learning', *IEEE Access*, 9, 153116 – 153125.

Zhang Xin and Wang, L. and W.T. and Z.D. and D.L., 2013, *Positioning Method for Automated Warehouses Based on RFID*, in M. Yang Yuhang and Ma (ed.), *Proceedings of the 2nd International Conference on Green Communications and Networks 2012 (GCN 2012): Volume 4*, 455–460, Springer Berlin Heidelberg, Berlin, Heidelberg.